

What Is the Mechanism of Catalysis of Ester Aminolysis by Weak Amine Bases? Comparison of Experimental Studies and Theoretical Investigation of the Aminolysis of Substituted Phenyl Esters of Quinoline-6- and -8-Carboxylic Acids

Helgi Adalsteinsson¹ and Thomas C. Bruice*

Contribution from the Department of Chemistry, University of California at Santa Barbara, Santa Barbara, California 93106

Received June 30, 1997

Abstract: The mechanisms of aminolysis of substituted phenylquinoline-8- and -6-carboxylates (Q-8 and Q-6) were evaluated using AM1 semiempirical and HF/6-31+G(d) ab initio quantum mechanical methods to study the ammonolyses of the model systems vinyl *cis*-3-(methyleneamino)acrylate (M1), *cis*-2-hydroxyvinyl *cis*-3-(methyleneamino)acrylate (M2), and vinyl *trans*-3-(methyleneamino)acrylate (M3). Both experimental and computational results support the formation of a tetrahedral intermediate in the reaction. The imine nitrogens of the Q-8, M1, and M2 esters are in position to catalyze aminolysis of the esters, whereas the imine nitrogens of the Q-6 and M3 esters are not. Ammonia attack on the M1 and M2 esters occurs at a hydrogen bonding distance above the imine nitrogen. This hydrogen bond prevails in the tetrahedral intermediate and during alkoxide departure. In a sequential step prior to diffusion apart, the very acidic N-protonated amide protonates the leaving alkoxide. Abstraction of the proton from the -NH₃⁺ substituent of the zwitterionic tetrahedral intermediate by imine nitrogen is thermodynamically highly unfavorable. The previously proposed proton slide mechanism involving catalysis by the imine nitrogen of intramolecular proton migration converting R-C(OR')(O⁻)(NH₃⁺) to R-C(OR')(OH)(NH₂) is not supported by the present study. The results of this study are fully consistent with the experimental observations for the aminolyses of substituted Q-8 and Q-6 esters.

Introduction

Early concepts of the mechanism of aminolysis of carboxylic acid esters have been reviewed by Bruice and Benkovic.² Dependent upon the nature of the leaving alkoxide or phenoxide, the aminolysis of an ester may resemble an S_N2 reaction with a tetrahedral transition state (eq 1) or a tetrahedral intermediate may be involved (eqs 2 and 3).³ The presence of tetrahedral intermediates was first established in ester hydrolysis by ¹⁸O exchange experiments.^{4,5} Tetrahedral intermediates in ester aminolysis reactions were first shown by the kinetic requirement of such intermediates in thioester aminolysis,⁴ and a tetrahedral intermediate in an acyl transfer reaction was later isolated by Rogers and Bruice.^{6,7} The existence of the stepwise reaction in eq 3 was established by Jencks from a study of the hydrazinolysis of phenyl acetate.⁸ The existence of tetrahedral intermediates has been shown in numerous acyl transfer reactions by a break in Brønsted or Hammett free energy plots due to a change in the rate-determining step from nucleophile attack for good leaving groups to leaving group expulsion for poor leaving groups.⁸

General-base catalysis of the aminolysis reaction was reported, independently, from the laboratories of Bruice,⁹ Bun-

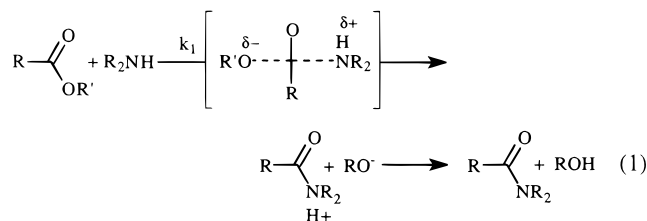
nett,¹⁰ and Jencks¹¹ in 1960 and subsequently explored.^{8,12–15} As seen in eqs 2 and 3, nucleophilic attack of amine on ester carbonyl can be concerted with proton removal by general base to provide an anionic tetrahedral intermediate (eq 2), or addition of amine to the ester carbonyl can provide a zwitterionic tetrahedral intermediate which can go on to products with general-base removal of the proton (eq 3). Only in the last case (eq 3) does one anticipate that the observed rate is proportional to the square of amine concentration ([R₂NH]²) at low [R₂NH], and that a linear relationship is seen between rate and [R₂NH] at higher amine concentrations.

Determination of the details of the mechanism of reactions composed of multiple steps by kinetic methods is often impossible: several different pathways can be kinetically equivalent, and kinetic studies give no information about reactions following the rate-determining step. Theoretical methods provide a way to compare different reaction pathways which may be kinetically equivalent.

The aminolysis of substituted phenyl quinoline-8-carboxylate esters (Q-8 esters) by various primary and secondary amines is subject to intramolecular catalysis by the quinoline nitrogen.^{16,17}

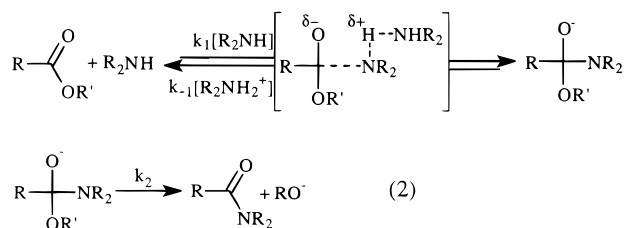
(1) In partial satisfaction of Ph.D. requirements.
(2) Bruice, T. C.; Benkovic, S. J. *Bioorganic Mechanisms*; W. A. Benjamin, Inc.: New York, 1966; Vol. 1.
(3) Williams, A. *Acc. Chem. Res.* **1989**, 22, 387.
(4) Fedor, L. R.; Bruice, T. C. *J. Am. Chem. Soc.* **1965**, 87, 4138.
(5) Bender, M. L.; Heck, H. d. A. *J. Am. Chem. Soc.* **1967**, 89, 1211.
(6) Rogers, G. A.; Bruice, T. C. *J. Am. Chem. Soc.* **1973**, 95, 4452.
(7) Rogers, G. A.; Bruice, T. C. *J. Am. Chem. Soc.* **1974**, 96, 2473.
(8) Blackburn, G. M.; Jencks, W. P. *J. Am. Chem. Soc.* **1968**, 90, 2638.
(9) Bruice, T. C.; Mayahi, M. F. *J. Am. Chem. Soc.* **1960**, 82, 3067.

(10) Bunnett, J. F.; Davis, G. T. *J. Am. Chem. Soc.* **1959**, 81, 665.
(11) Jencks, W. P.; Carriolo, J. *J. Am. Chem. Soc.* **1960**, 82, 675.
(12) Jencks, W. P.; Gilchrist, M. *J. Am. Chem. Soc.* **1966**, 88, 104.
(13) Bruice, T. C.; Donzel, A.; Huffman, R. W.; Butler, A. R. *J. Am. Chem. Soc.* **1967**, 89, 2106.
(14) Huffman, R. W.; Donzel, A.; Bruice, T. C. *J. Am. Chem. Soc.* **1967**, 89, 1973.
(15) Bruice, T. C.; Hegarty, A. F.; Felton, S. M.; Donzel, A.; Kundu, N. *J. Am. Chem. Soc.* **1970**, 92, 1370.
(16) Bruice, P. Y.; Bruice, T. C. *J. Am. Chem. Soc.* **1974**, 96, 5523.
(17) Bruice, P. Y.; Bruice, T. C. *J. Am. Chem. Soc.* **1974**, 96, 5533.



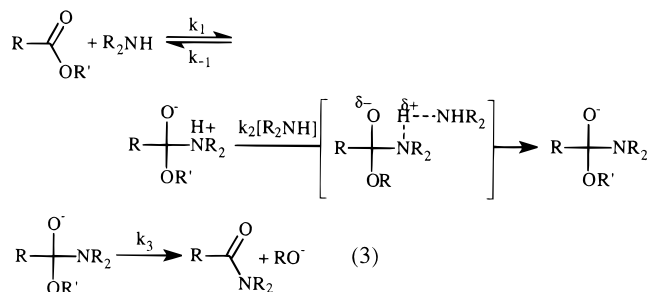
Yielding the observed pseudo-first order rate constant

$$k_{\text{obs}} = k_1[\text{R}_2\text{NH}]$$



Steady state assumption provides

$$k_{\text{obs}} = \frac{k_1 k_2 [\text{R}_2\text{NH}]^2}{k_{-1} [\text{R}_2\text{NH}_2^+] + k_2}$$

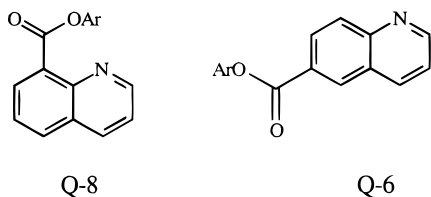


Steady state assumption provides the observed

$$k_{\text{obs}} = \frac{k_1 k_2 [\text{R}_2\text{NH}]^2}{k_{-1} + k_2 [\text{R}_2\text{NH}]}$$

pseudo-first order rate constant (k_{obs})

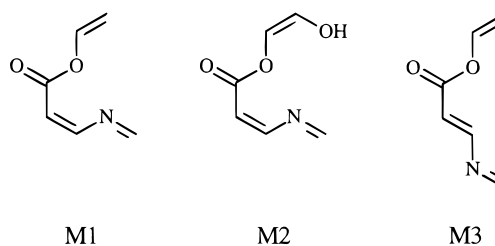
Aminolysis of Q-8 esters occurs up to 200-fold faster than aminolysis of quinoline-6-carboxylate esters (Q-6 esters), in



which the quinoline nitrogen cannot serve as catalyst. It should be noted that the uncatalyzed reactions of hydroxide with Q-6 and Q-8 esters occur at roughly the same rate (Q-6 esters react 5–6 times faster than Q-8 esters) and the electron densities at the ester carbonyl of Q-8 and Q-6 esters are comparable by MO calculations.¹⁶ No solvent kinetic isotope effect was observed for the aminolysis of Q-8 esters, and the quinoline nitrogen remains an efficient catalyst even when the amine moiety of the tetrahedral intermediate is 7 pK_a units a stronger

base than the quinoline nitrogen.¹⁶ Three plausible, but experimentally indistinguishable, mechanisms may be considered for the intramolecular catalysis. The first of these is proton abstraction by the quinoline nitrogen and rapid subsequent leaving group expulsion (Scheme 1). The second possibility is that the amine proton does not get abstracted until after leaving group expulsion; the mode of catalysis is then electrostatic stabilization of the positive charge on the amine nitrogen by the quinoline nitrogen (Scheme 2). The third mechanistic pathway was proposed by the authors of the experimental study.¹⁶ It consists of electrostatic stabilization by the quinoline nitrogen lone pair during proton transfer from the protonated amine moiety of the tetrahedral intermediate to the alkoxide oxygen to form an uncharged tetrahedral intermediate (Scheme 3). The authors coined the term “proton slide catalysis” to describe this reaction pathway.

This paper revisits the aminolysis reactions of the substituted phenyl quinoline-6- and -8-carboxylate esters (Q-6 and Q-8 esters) using theoretical methods to identify the preferred mode of catalysis. The model systems examined in this study, M1, M2, and M3 esters, were designed to represent the important



features of Q-8 and Q-6 esters while still enabling semiempirical and ab initio aqueous solvation calculations to be finished in a reasonable amount of time. The M1 and M2 esters were devised to study the mode of catalysis and the effects of different leaving groups on the reaction barrier. The added *cis*-hydroxyl group on M2 ester is in position to stabilize the leaving group through hydrogen bonding as might water solvent. The pK_a of the enediol leaving group of M2 has been estimated to be 10–11,¹⁸ making it a suitable model for a phenol leaving group. The M3 ester was devised to examine the progress of the uncatalyzed ammonolysis reaction, thereby mimicking the aminolysis reactions of Q-6 esters. The electron densities at the carbonyl carbons of the M1, M2, and M3 esters are virtually identical by AM1/SM2.1 calculations.

Experimental Section

To simulate the quinoline moiety of the Q-8 and Q-6 esters, rotation around the C3=C4–N5=C6 bonds of the model esters was constrained (the constrained bonds are shown for M1 ester in Chart 1), thereby forcing all the atoms in the imine chain to lie in the same plane. Otherwise, no constraints were used in the identification of ground state or transition state structures.

All three quinoline ester model systems, M1, M2, and M3, were studied by semiempirical orbital calculations using the AM1 semiempirical method¹⁹ with the SM2.1 aqueous solvation model²⁰ (AM1/SM2.1) provided in the program Ampac 5.0.²¹ Approximate transition states were located by AM1/SM2.1 reaction coordinate calculations; exact transition state geometries were verified by vibrational analysis and IRC calculations. Additionally, ab initio molecular orbital calculations were carried out on the reactions of model system

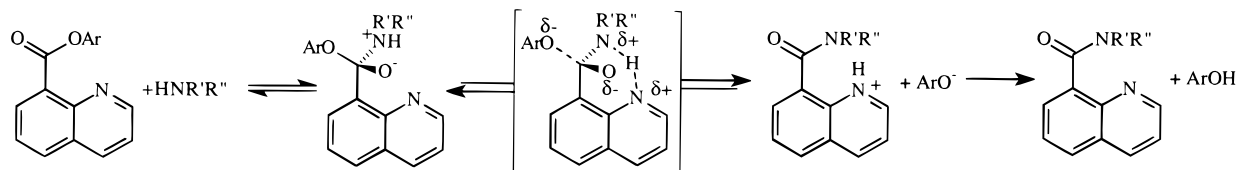
(18) Gerlt, J. A.; Gassman, P. G. *J. Am. Chem. Soc.* **1993**, *115*, 11552.

(19) Dewar, M. J. S.; Zoebisch, E. G.; Healy, E. F.; Stewart, J. J. P. *J. Am. Chem. Soc.* **1985**, *107*, 3902.

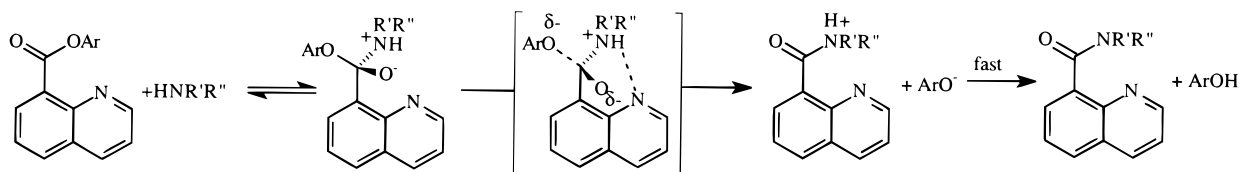
(20) Cramer, C. J.; Truhlar, D. G. *J. Comput.-Aided Mol. Des.* **1992**, *6*, 629.

(21) *Ampac 5.0*, Semichem, 7128 Summit, Shawnee, KS 66126, 1994.

Scheme 1



Scheme 2



Scheme 3

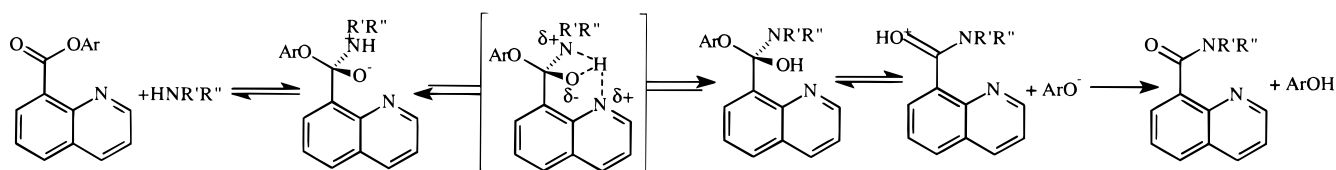
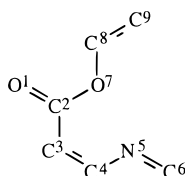


Chart 1



M1 at the HF/6-31+G(d) level of theory using two different aqueous solvation simulations: (i) the self-consistent isodensity polarized continuum model (SCI-PCM)^{22–24} provided in Gaussian 94²⁵ and (ii) the PS-Solv ab initio aqueous solvation routine²⁶ in the PS-GVB suite of programs.²⁷ The reactions studied for ammonolysis of the M2 and M3 esters were limited to those reactions found to be feasible for the ammonolysis of the M1 ester.

In the intramolecular catalysis of the ammonolysis reactions of the M1, M2, and M3 esters (and substituted Q-8 and Q-6 esters) there is no change in the number of degrees of freedom or number of atoms participating in each reaction step except for the association of reactants and the dissociation of products. All the transition states and tetrahedral intermediates being compared are single-molecule systems; differences in entropy for the different reaction mechanisms should thus be minimal, and the calculated activation barriers should be equal to the free energy of activation of the corresponding reaction step ($\Delta\Delta H^\ddagger \approx \Delta\Delta G^\ddagger$),

(22) Wiberg, W. B.; Keith, T. A.; Frisch, M. J.; Murcko, M. *J. Phys. Chem.* **1995**, *99*, 9072.

(23) Wiberg, K. B.; Rablen, P. R.; Rush, D. J.; Keith, T. A. *J. Am. Chem. Soc.* **1995**, *117*, 42.

(24) Wiberg, K. B.; Castejon, H.; Keith, T. A. *J. Comput. Chem.* **1996**, *17*, 185.

(25) Frisch, M. J.; Trucks, G. W.; Schlegel, H. B.; Gill, P. M. W.; Johnson, B. G.; Robb, M. A.; Cheeseman, J. R.; Keith, T.; Petersson, G. A.; Montgomery, J. A.; Raghavachari, K.; Al-Laham, M. A.; Zakrzewski, V. G.; Ortiz, J. V.; Foresman, J. B.; Cioslowski, J.; Stefanov, B. B.; Nanayakkara, A.; Challacombe, M.; Peng, C. Y.; Ayala, P. Y.; Chen, W.; Wong, M. W.; Andres, J. L.; Replogle, E. S.; Gomperts, R.; Martin, R. L.; Fox, D. J.; Binkley, J. S.; Defrees, D. J.; Baker, J.; Stewart, J. P.; Head-Gordon, M.; Gonzalez, C.; Pople, J. A. *Gaussian 94 (Revision D.4)*, Gaussian Inc., Pittsburgh, PA, 1995.

(26) Tannor, D. J.; Marten, B.; Murphy, R.; Friesner, R. A.; Sitkoff, D.; Nicholls, A.; Ringnalda, M.; Goddard, W. A., III; Honig, B. *J. Am. Chem. Soc.* **1994**, *116*, 11875.

(27) Ringalda, M. N.; Langois, J.-M.; Murphy, R. B.; Greeley, B. H.; Cortis, C.; Russo, T. V.; Marten, B.; Donnelly, R. E., Jr.; Pollard, W. T.; Cao, Y.; Muller, R. P.; Mainz, D. T.; Wright, J. R.; Miller, G. H.; Goddard, W. A., III.; Friesner, R. A. *PS-GVB v2.3*, Schrödinger, Inc., 1996.

enabling the determination of favorable pathways and rate-determining steps. Additionally, all the model systems studied follow the same reaction path and have very similar ground state and transition state geometries (vide infra), which further validates the approximation above.

Results and Discussion

Both the experimental work on aminolysis of substituted phenylquinoline 6- and 8-esters (Q-8 and Q-6 esters) and the computational results from this study support the existence of tetrahedral intermediates.¹⁷ Thus, the present study does not deal with ester aminolysis by concerted S_N2 amine attack and alkoxide expulsion (eq 1). The kinetic data on the aminolyses of Q-8 and Q-6 esters is not sufficient to resolve the catalytic pathway; several kinetically equivalent reaction pathways can be contrived.

A Review of the Aminolysis Reactions of Substituted Phenyl Q-6 and Q-8 Esters. As stated previously, the aminolysis reactions were shown to involve at least one intermediate. This conclusion was based on the break in the Hammett plots of the second-order rate constants for reaction of amine and substituted phenyl esters of Q-8 and Q-6. The Hammett plots for reactions of methylamine with substituted Q-8 and Q-6 esters are provided in Figure 1a.¹⁷ For substituted phenoxide leaving groups with substituent σ less than ~ 0.8 , the second-order rate constants for aminolysis of Q-8 esters exceed the second-order rate constants determined for Q-6 esters (Figure 1). The methylaminolysis reaction is about 100 times more facile for the *p*-methoxyphenyl Q-8 ester than for the *p*-methoxyphenyl Q-6 ester (the *p*-methoxy substituent has $\sigma = -0.27$). When the substituent constant σ exceeds ~ 1.0 , the second-order rate constants for the aminolysis of Q-8 esters become independent of the substituent, resulting from a change in the rate-determining step, presumably from departure of the leaving group to nucleophilic attack.

When σ of the para substituent on the leaving phenoxides of Q-8 esters is less than ~ 1.0 , the slope ρ of the Hammett plot is ~ 2.0 and ~ 1.5 for aminolysis with methylamine and pyrrolidine, respectively (Figure 1). The reactions of the corresponding Q-6 esters with methylamine or pyrrolidine have $\rho \approx 3$. No deuterium solvent kinetic isotope effect was observed for the

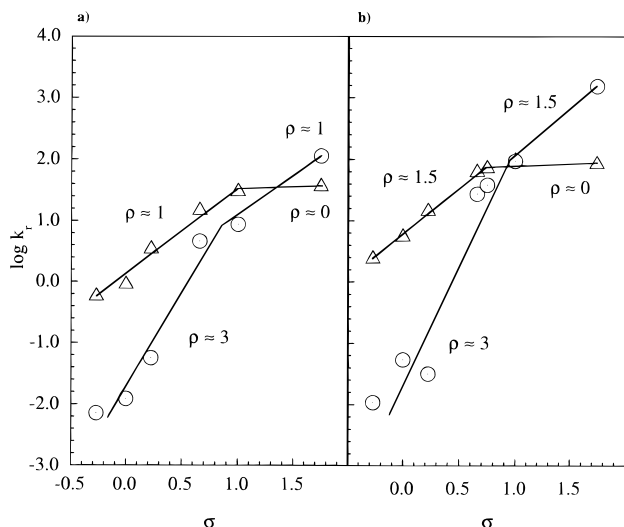
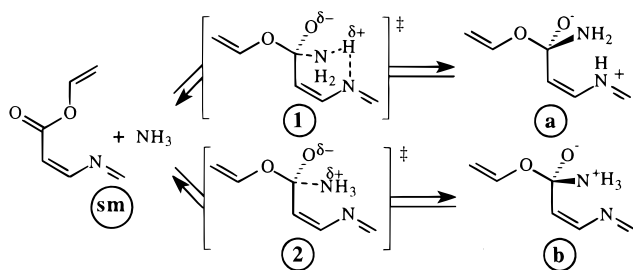


Figure 1. Hammett plots of the experimental second-order rate constant for the nucleophilic attack of methylamine (a) and pyrrolidine (b) on substituted Q-8 (Δ) and Q-6 (\circ) esters. Data from ref 17.

Scheme 4



second-order reaction of glycine with *p*-chlorophenyl and 2,4-dinitrophenyl Q-6 and Q-8 esters.¹⁷ Leaving group expulsion is rate determining in the reaction of glycine with *p*-chlorophenyl Q-8 ester while amine attack is rate determining in the reaction of glycine with 2,4-dinitrophenyl Q-8 ester.¹⁷ Thus, there is no proton transfer in either of the observed rate-determining steps of the bimolecular reaction; proton transfer from the attacking amine must therefore occur either in an intermediate step or after phenoxide expulsion. The aminolysis reactions of substituted phenyl Q-6 esters were found to be exclusively second order in amine concentration for four out of six substituted phenyl esters examined. Only for one of seven substituted phenyl Q-8 esters was aminolysis second order in amine. Thus, the aminolyses of Q-6 esters are subject to external general-base catalysis by a second molecule of amine while the aminolyses of the Q-8 esters are less so due to the competing intramolecular assistance by the neighboring quino-line nitrogen.

Computational Results. Two plausible initial reaction steps for ammonolysis of the M1 ester are shown in Scheme 4. The first, which passes through transition state **1** to product **a**, is ammonia attack with concerted proton abstraction. The experimental investigation of the aminolyses of Q-8 and Q-6 esters (vide supra) does not support ammonia attack with concerted proton abstraction, but the reaction mechanism is examined here to verify the reliability of the calculations. The second reaction considered is ammonia attack without proton abstraction, giving the zwitterionic tetrahedral intermediate **b**. In the reaction coordinate of Figure 2, the semiempirical AM1/SM2.1 aqueous heats of activation are provided for the reaction pathways shown in Scheme 4. The energy barriers are 32 kcal/mol for ammonia attack with concerted proton abstraction and 18 kcal/mol for

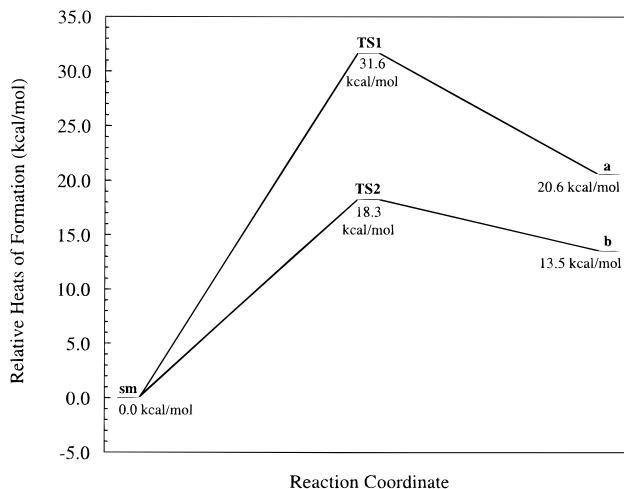


Figure 2. A comparison of the AM1/SM2.1 energies for transition state formation for concerted amine attack with proton abstraction (**TS1**) and stepwise amine attack (**TS2**) on M1 ester. The labels in this figure correspond to the labeled structures in Scheme 4.

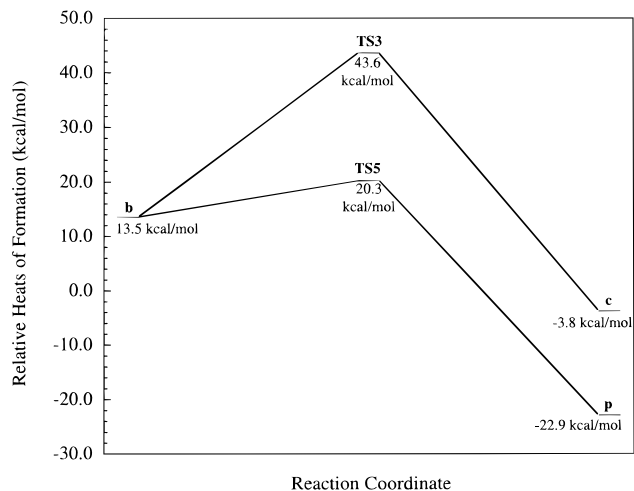
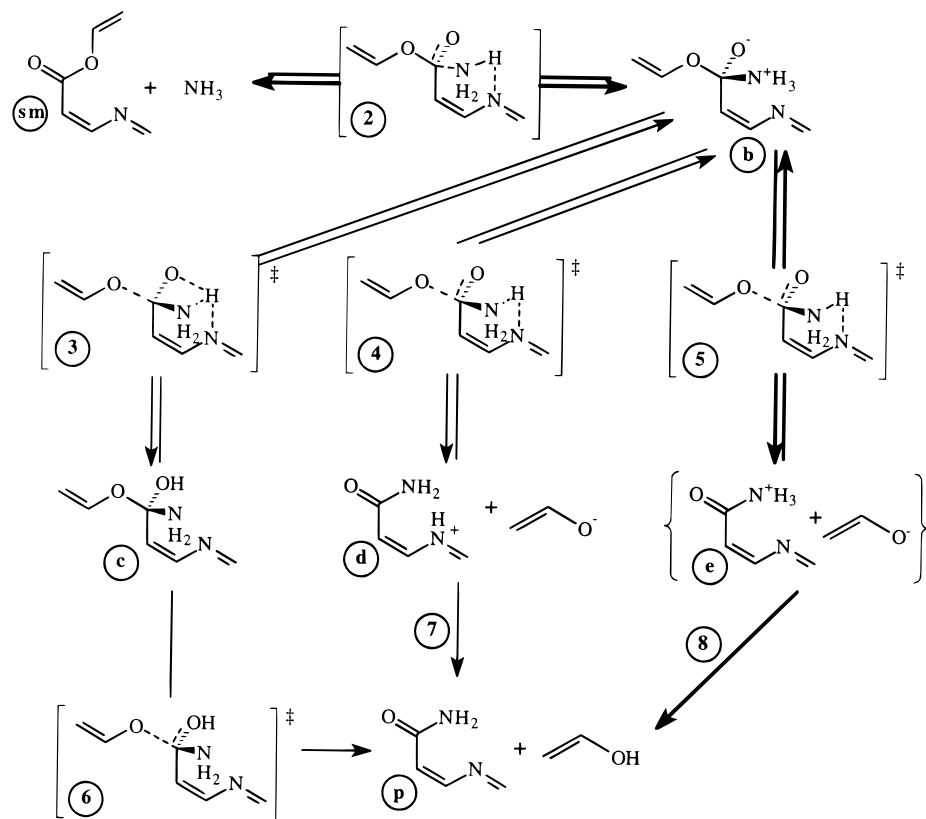


Figure 3. A comparison of the AM1/SM2.1 energies for proton slide from amine nitrogen to alkoxide oxygen (**TS3**) and leaving group expulsion with a proton on an amine nitrogen (**TS5**) followed by rapid proton transfer from the protonated amide to the leaving alkoxide for the M1 ester. The labels in this figure correspond to the labeled structures in Scheme 5.

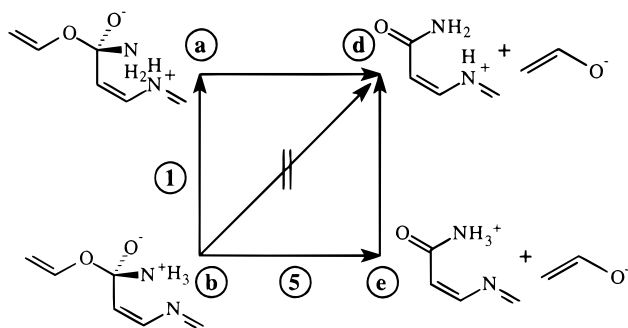
direct ammonia attack without proton abstraction, and the barriers for the reverse reactions are 11.0 and 4.7 kcal/mol, respectively. In accordance with the experimental evidence for the reactions of the Q-8 and Q-6 esters,¹⁷ ammonia attack with simultaneous proton abstraction is found to be unfavorable (Scheme 4, **sm** \rightleftharpoons **a**) compared with the mechanism not involving proton transfer in the initial step (Scheme 4, **sm** \rightleftharpoons **b**).

The pathways following ammonia attack in Scheme 5 are now considered. The proton slide reaction (**b** \rightleftharpoons **c**) and direct alkoxide expulsion (**b** \rightleftharpoons **e**) can be examined in a straightforward manner and are shown in Figure 3, but the concerted alkoxide expulsion with proton transfer (**b** \rightleftharpoons **d**) requires the use of a More O'Ferrall diagram (Scheme 6).²⁸ Alkoxide expulsion with simultaneous proton transfer to the imine nitrogen can be eliminated when the relative AM1/SM2.1 heats of formation of intermediates **a** and **e** are compared to the value for intermediate **b**. Intermediate **e** is appreciably lower in energy than intermediate **b** (difference in relative AM1/SM2.1 heats of formation (ΔH_c^{e-b}) is -3.9 kcal/mol) while intermediate **a**

Scheme 5



Scheme 6



is of greater energy than **b** (difference in relative AM1/SM2.1 heats of formation (ΔH_c^{a-b}) is 7.1 kcal/mol). Thus, concerted reactions of Scheme 6 are shown in Figure 4.

After alkoxide expulsion, the protonated amide and alkoxide form an ion complex, which then undergoes rapid sequential proton transfer to yield the products *cis*-3-(methyleneamino)acrylamide and vinyl hydroxide (Scheme 7). This proton transfer has a low activation barrier (3.64 kcal/mol), and the reassociation of alkoxide and protonated amide is disfavored ($\Delta H^\ddagger = 10.0$ kcal/mol).

The favored reaction pathway for ammonolysis is shown using boldface arrows in Scheme 5. The energy profiles for the ammonolyses of the M1 and M2 esters are shown in Figure 5, and the energy profile for the ammonolysis of the M3 ester is compared to the energy profile for the M1 ester in Figure 6. The calculated relative heats of formation for the ammonolysis of the M1, M2, and M3 esters are shown in Table 1.

The mode of catalysis can be determined by comparing the energy profiles and the transition state and intermediate

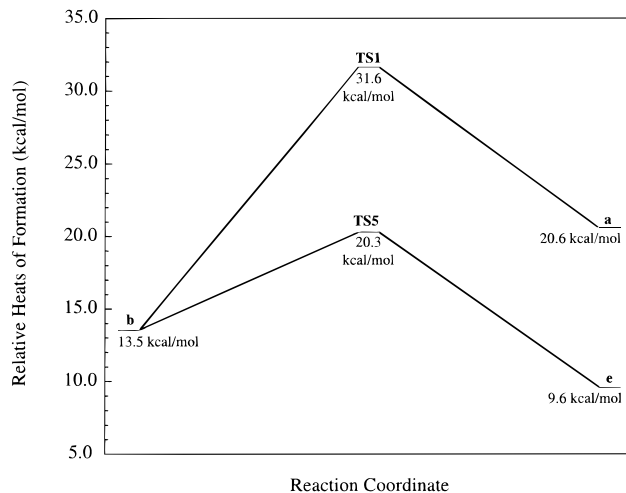


Figure 4. A comparison of the AM1/SM2.1 energies for proton abstraction followed by leaving group transfer from amine nitrogen to imine nitrogen (TS1) and leaving group expulsion followed by proton transfer from amide nitrogen to imine nitrogen (TS5) used to determine if concerted proton abstraction and leaving group expulsion is feasible for the M1 ester. The labels used in this figure correspond to the labeled structures in Scheme 6.

geometries for the three model systems. The intermediate and transition state structures for model systems M1 through M3 are provided in Figures 7–9. For the models M1 and M2, the nucleophilic NH_3 approaches the ester carbonyl carbon by passing over the sp^2 electron pair of the substrate imine nitrogen, and in the transition state the substrate imine nitrogen is hydrogen bonded to the attacking NH_3 ($\text{H}\cdots\text{N}$ distance 2.13 Å, Figure 7a,b). In the resulting tetrahedral intermediate structures, the protonated amino group is stabilized by hydrogen bonding to the imine nitrogen ($\text{H}\cdots\text{N}$ distance 2.0 Å, Figure 8a,b). The hydrogen bond between imine nitrogen and the $-\text{NH}_3^+$ moiety

(29) Jencks, W. P. *Chem. Rev.* **1972**, *72*, 705.

Scheme 7

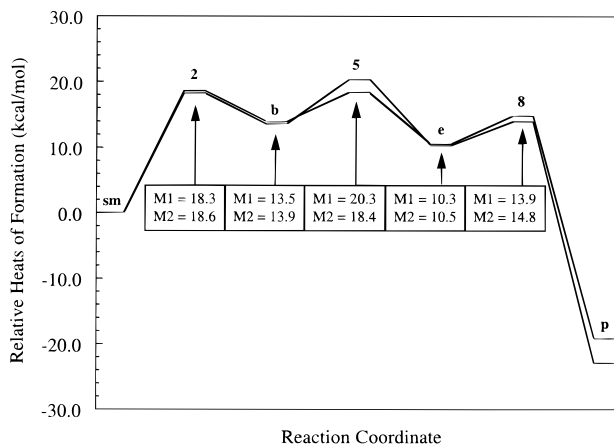
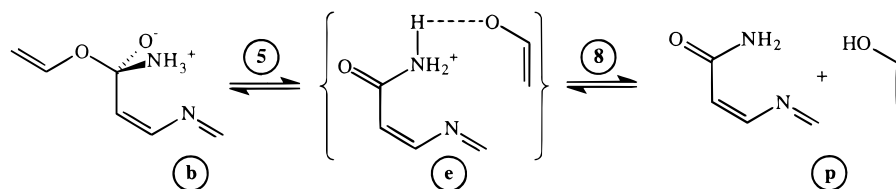


Figure 5. A comparison of the AM1/SM2.1 energies for ammonolysis of M1 and M2 esters. The reaction examined in this figure is shown in Scheme 5, and the relative heats of formation of the reaction intermediate and transition states are shown in Table 1.

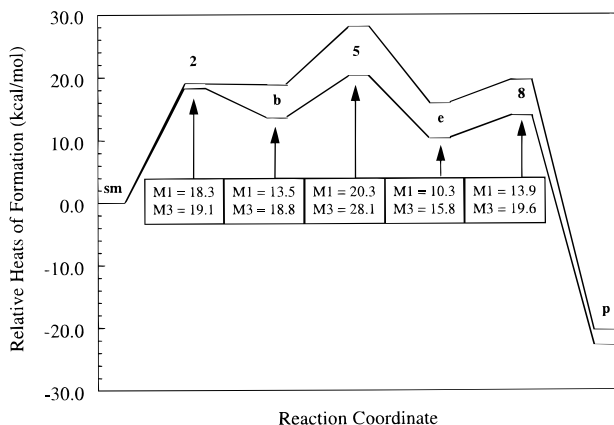


Figure 6. A comparison of the AM1/SM2.1 energies for ammonolysis of M1 and M3 esters. The reaction examined in this figure is shown in Scheme 5, and the relative heats of formation of the reaction intermediate and transition states are shown in Table 1.

Table 1. Relative Heats of Formation (kcal/mol) Found for the Favored Reaction in Scheme 5

	M1 ester	M2 ester	M3 ester
starting materials (sm)	0.00	0.00	0.00
ammonia attack transition state (2)	18.27	18.60	19.08
tetrahedral intermediate (b)	13.54	13.86	18.78
alkoxide expulsion transition state (5)	20.30	18.42	28.12
products (p)	-22.90	-19.21	-20.41

remains intact in the transition state for alkoxide leaving (Figure 9a,b) which is followed by rapid synchronous proton transfer from protonated amide nitrogen to leaving alkoxide. In solution, the proton transfer would be prior to solvent separation of the ion pair. Such catalysis is not possible with M3 (Figures 7c, 8c, and 9c). A comparison of the reaction profiles of model systems M1 and M3 (Figure 6) reveals that intramolecular catalysis by the imine nitrogen is by stabilization of the

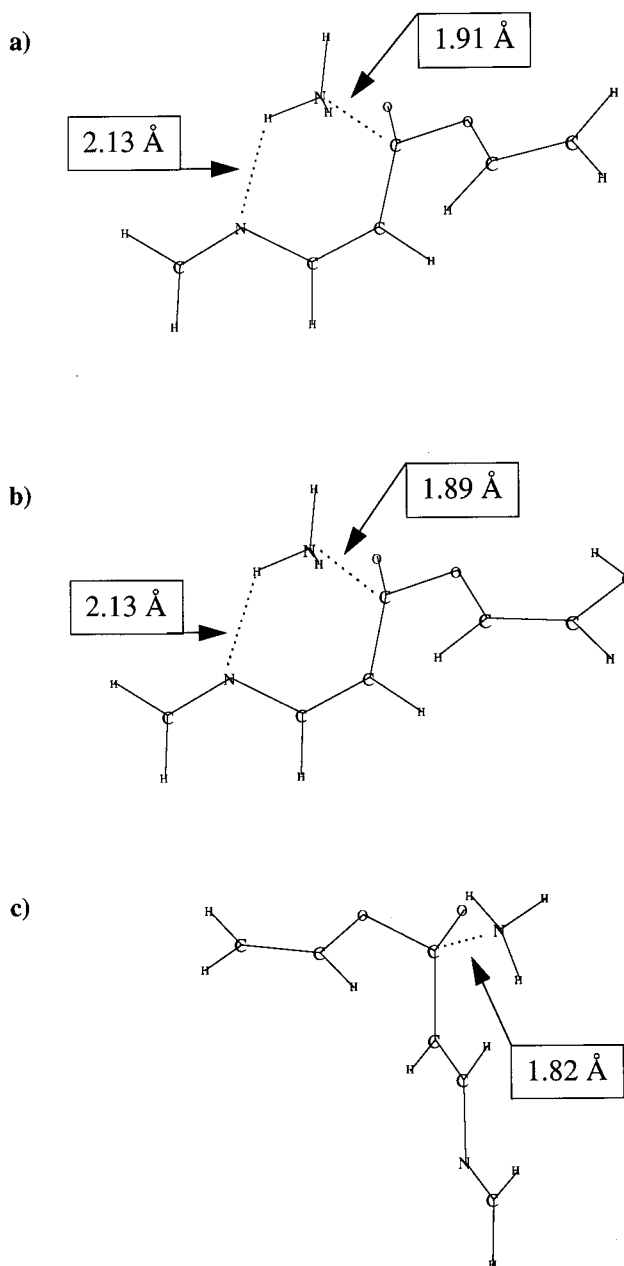


Figure 7. Transition state geometries found for ammonia attack on M1 (a), M2 (b), and M3 (c) esters. The N...C transition state distances and N...H hydrogen bond distances found by AM1/SM2.1 semiempirical calculations are shown next to the dotted lines used to indicate the bonds.

tetrahedral intermediate and the transition state for alkoxide expulsion through hydrogen bonding.

Comparison of Computational and Experimental Results. The kinetic findings on the aminolyses of Q-8 esters (vide supra)¹⁷ are in excellent accordance with the intramolecular catalytic pathway we have found most favorable for the M1 and M2 esters and the results with the M3 ester. Since the

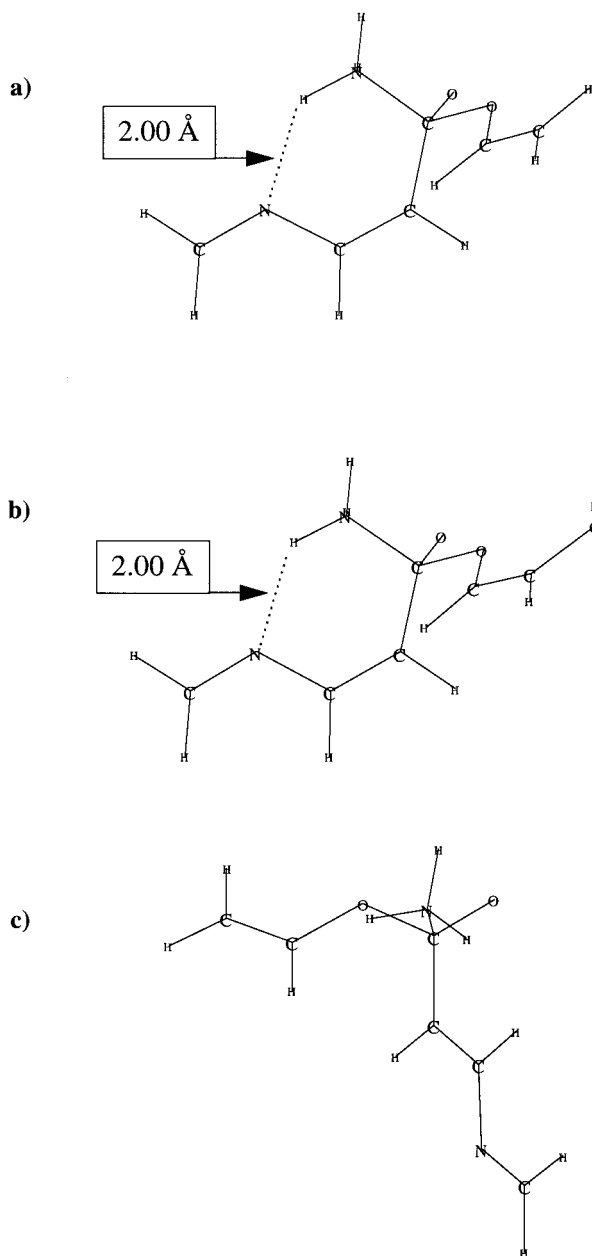


Figure 8. Tetrahedral intermediate geometries found for ammonia attack on M1 (a), M2 (b), and M3 (c) esters. The N...H hydrogen bonding distances found by AM1/SM2.1 semiempirical solvation calculations are shown next to the dotted line used to indicate the hydrogen bonds.

heats of formation of the transition states for NH_3 attack on the M1 and M2 esters are equal, ρ is zero when ammonia attack is rate determining. According to AM1/SM2.1 calculations, the leaving alcohols of the M1 and M2 esters have $\Delta\text{p}K_a \approx 3$. The slope of the correlation between $\log k'_2$ and $\text{p}K_a$ is -0.34 for the ammonolysis of M1 and M2 esters. This value may be compared to a Brønsted slope of -0.56 for the experimentally measured rate of reaction of methylamine with substituted Q-8 esters with σ less than 0.8 (phenoxide expulsion is rate determining). This is, to say the least, an excellent correlation between theory and experiment. The greater rate constants for aminolysis of substituted Q-8 esters compared to Q-6 esters with poor leaving groups reflects the catalytic role of the quinoline nitrogen in the reactions. By comparing the ammonolysis reactions of the M1 and M3 esters (Figure 9), it becomes apparent that the imine nitrogen acts to stabilize the tetrahedral

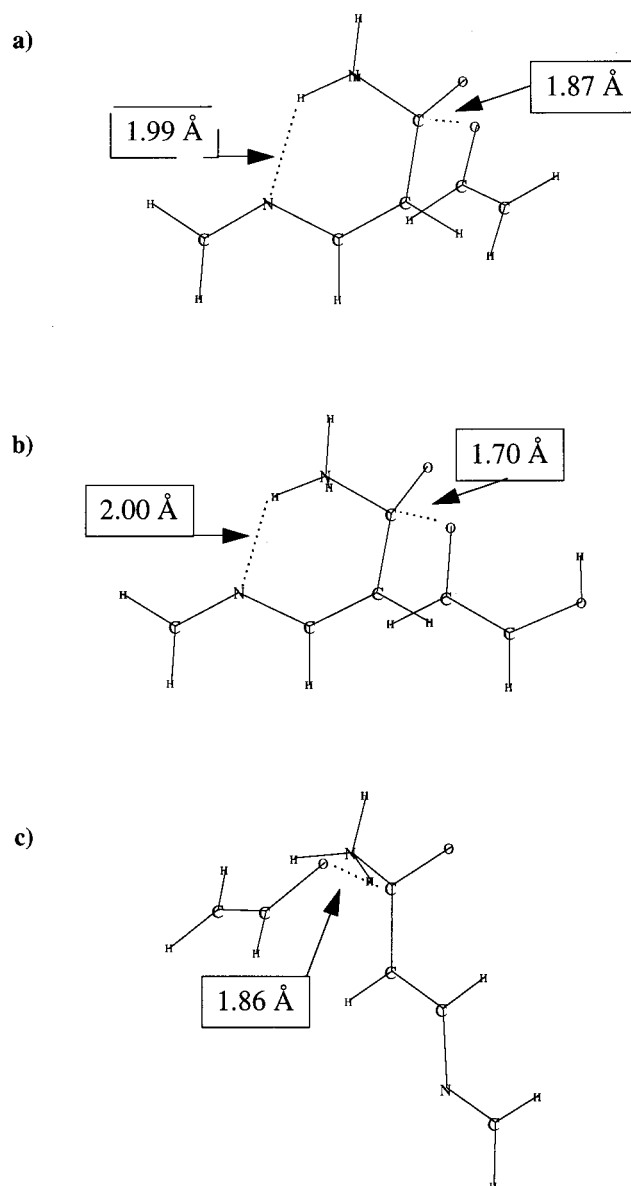


Figure 9. Transition state geometries found for alkoxide expulsion following ammonia attack on M1 (a), M2 (b), and M3 (c) esters. The O...C transition state distances and N...H hydrogen bond distances found by AM1/SM2.1 semiempirical solvation calculations are shown next to the dotted lines used to indicate the bonds.

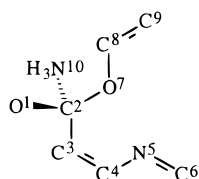
intermediate and the transition state of alkoxide expulsion, while the effect of the imine nitrogen on ammonia attack is negligible. The measured rate constants for reaction of amines with substituted Q-8 esters are greater by up to 200-fold compared to the rate constants for the corresponding Q-6 esters. The reaction of Q-6 esters with hydroxide proceeds 5–6 times faster than the reactions of corresponding Q-8 esters. Using the hydrolysis reaction to adjust the uncatalyzed reaction rate for the Q-6 and Q-8 esters, the rate enhancement due to intramolecular catalysis is 1000–1200-fold. The rate difference calculated for the ammonolysis reactions of the M1 and M3 esters is 1200-fold, in perfect correlation with the experimental observations of the aminolysis reactions of Q-8 and Q-6 esters. In the computational model, the hydrogen-bonded proton is not abstracted from the amine until after alkoxide expulsion; this is in accordance with the inability to observe a deuterium solvent kinetic isotope effect in the aminolysis of the Q-8 esters, regardless of whether amine attack or phenoxide expulsion is rate determining.

Table 2. Comparison of the Relative Heats of Formation of Transition States and Tetrahedral Intermediate for the Aminolysis Reaction of the M1 Ester Found by Semiempirical and *ab Initio* MO Methods^a

theoretical method (energies in kcal/mol)	starting materials	TS for NH ₃ attack	tetrahedral intermediate	TS for RO ⁻ expulsion	products
AM1/SM2.1	0	18.3	13.5	20.3	-22.9
PS-Solv 6-31+G(d)	0	9.8	-2.3	9.6	-6.0
SCI-PCM 6-31+G(d)	0	21.7	20.7	DNC	-14.5

^a DNC = did not converge.**Table 3.** Transition-State and Intermediate Geometries Found for the Ammonolyses of M1, M2, and M3 Esters^a

bond length or angle (see Chart 2)	ammonia attack transition state			tetrahedral intermediate			alkoxide expulsion transition state		
	M1	M2	M3	M1	M2	M3	M1	M2	M3
<i>r</i> _{C2-O1} (Å)	1.26	1.26	1.27	1.31	1.30	1.29	1.26	1.29	1.26
<i>r</i> _{C2-O7} (Å)	1.43	1.42	1.42	1.48	1.48	1.46	1.87	1.70	1.86
<i>r</i> _{C2-N10} (Å)	1.91	1.89	1.82	1.57	1.58	1.61	1.51	1.53	1.51
<i>θ</i> _{O1-C2-O7} (deg)	109.0	109.5	108.5	106.1	106.0	106.4	100.3	104.5	100.2
<i>θ</i> _{O1-C2-N10} (deg)	103.0	103.3	104.1	108.1	108.8	108.1	115.0	112.2	115.0

^a The labels in the table are relative to Chart 2, with "r" indicating a bond distance and "θ" indicating a bond angle.**Chart 2**

Ab initio Calculations. The computed reaction coordinate for the favored (boldface arrows) reaction sequence of Scheme 5 was calculated for M1 using SCI-PCM and PS-Solv *ab initio* solvation calculations at the HF/6-31+G(d) level of theory (Table 2). All three theoretical methods predict that a tetrahedral intermediate should be formed in this reaction, and both AM1/SM2.1 semiempirical calculations and PS-Solv HF/6-31+G(d) calculations predict that the transition states for ammonia attack and leaving group expulsion for the M1 model system should be of comparable energy. Perusal of Table 2 shows that the activation energy barriers for ammonia attack using SCI-PCM HF/6-31+G(d) and AM1/SM2.1 are comparable whereas the tetrahedral intermediate is less stable according to SCI-PCM HF/6-31+G(d) results than by AM1/SM2.1 semiempirical findings, and PS-Solv HF/6-31+G(d) gives an unreasonably stable tetrahedral intermediate. We failed to find a transition state for alkoxide expulsion by use of SCI-PCM *ab initio* calculations.

Transition State and Intermediate Geometries. The geometries of transition states (Figures 7 and 9) and tetrahedral intermediates (Figure 7) found by AM1/SM2.1 semiempirical calculations for the ammonolysis of M1 and M2 esters are now considered. While attacking the ester, the ammonia is hydrogen bonded to the imine nitrogen (hydrogen bonding distance 2.0 Å, Figure 6), and during alkoxide expulsion this hydrogen bond remains in place at 2.0 Å (Figure 7). The transition state geometries for ammonia attack on the model systems M1 and M2 are almost identical (Figure 6), but the transition state geometry for alkoxide expulsion in the M2 model system is 0.17 Å earlier than that found for the M1 model system (Figure 8). The key bond distances and angles in the transition states and tetrahedral intermediate, as found by AM1/SM2.1 calculations, are given in Table 3. Identifications for the labels in Table 3 are given in Chart 2. The geometries of the transition states for ammonia attack found by SCI-PCM and PS-Solv *ab initio* aqueous solvation calculations are tighter (more similar to gas-

phase geometries) than those found by AM1/SM2.1 semiempirical aqueous solvation calculations. This difference can be attributed to the exclusion of entropy of solvation in the *ab initio* solvation models.

On the basis of the correlation between this mechanism and the experimental evidence for the aminolysis reactions of substituted phenylquinoline-8-carboxylate esters, it is reasonable to assume that the aminolysis reactions of substituted phenyl Q-8 esters follow the same reaction mechanism as the M1 and M2 esters.

Conclusion

The lowest energy pathway found for the ammonolysis of M1 and M2 esters in the semiempirical AM1/SM2.1 solvation calculations involves a zwitterionic tetrahedral intermediate {R-C(OR')(O⁻)(NH₃⁺)}. This is supported by PS-Solv and SCI-PCM 6-31+G(d) *ab initio* calculations. Attack of ammonia occurs at a hydrogen bonding distance of 2.13 Å above the ester imine. This hydrogen bond does not lower the barrier for ammonia attack, but stabilizes the tetrahedral intermediate and transition state during alkoxide (O⁻R') departure. The protonated amide formed upon alkoxide expulsion is stabilized by a 1.99 Å hydrogen bond to the imine nitrogen. In a sequential step prior to diffusion apart, the leaving alkoxide is protonated by the protonated amide {R-C(=O)-NH₃⁺} (Scheme 5).

The previously proposed proton slide mechanism^{16,17} of catalysis involved intramolecular proton migration by quinoline nitrogen, converting R-C(OR')(O⁻)(NH₃⁺) to R-C(OR')(OH)(NH₂). This mechanism is not supported by the present study. In the proton slide transition state, the distance between the proton being transferred from the protonated amine of the tetrahedral moiety to the alkoxide and the imine nitrogen is in excess of 2.8 Å. This distance is too large for the imine nitrogen to significantly stabilize the transition state. It is reasonable, on the basis of the experimental results from the aminolysis reactions of substituted Q-8 esters, to assume that the aminolysis reactions of Q-8 esters follow the same reaction mechanism as the ammonolysis of M1 and M2 esters.

Acknowledgment. This work was supported by a grant from the National Institutes of Health. We thank the ONR for support of our computational facility.